International Conference on Non-conventional Materials and Technologies
NOCMAT 2022

MECHANICAL AND STRUCTURAL ANALYSIS OF FLAT TERRY FABRICS

Mariana Costa Laktim, Minas Gerais State University (ED-UEMG), Brazil, marilaktim@gmail.com
Juan Camilo Adrada Molano, University of São Paulo (FZEA – USP), Brazil, camiloadrada@usp.br
Rafael Henrique Filomeno, University of São Paulo (FZEA – USP), Brazil, rafaelfilomeno@usp.br
Júlia Baruque-Ramos, University of São Paulo (EACH – USP), Brazil, jbaruque@usp.br
Holmer Savastano Junior, University of São Paulo (FZEA – USP), Brazil, holmersj@usp.br
Raul Fangueiro, University of Minho (Azurém - UMinho), Portugal, rfangueiro@dem.uminho.pt
Rita de Castro Engler, Minas Gerais State University (ED – UEMG), Brazil, rita.engler@gmail.com

ABSTRACT

This research aimed at the characterization of terry fabrics (Material 1 - Egyptian cotton and Material 2 - upland cotton) for potential as reinforcing elements in engineered composites. Microscopy, tensile tests, and DIC were carried out. Material 1 presented tighter ligament, lower tensile stress (weft: 3.5 MPa; warp: 4.9 MPa), modulus of elasticity (weft: 4.0 MPa; warp: 3.4 MPa), and tear strength (weft: 94.4 N; warp: 48.5 N) and inferior central breaking points in the weft direction and the upper jaws in the warp direction about Material 2. Composites incorporating terry fabrics and other tests should still be realized.

KEYWORDS
Terry Fabrics; DIC; Tensile Test; Textile Application; Cotton.

INTRODUCTION

In the textile industry, research for fabric development aims to respond to thermal, chemical, mechanical, and electrical stimuli, among others. These material characteristics give rise to new technological applications. Flat terry fabric is a textile product made with loops (piles) on one or both sides, usually covering the entire surface or strips. The production of terry fabrics is a complex process with three yarn (or thread) systems: ground warp, pile warp, and weft (or filling). The ground warp threads have higher tensile, while the pile warp threads have much lower tensile and consequently greater length, to create the terry loops through the special movement of the loom's reed with weak and strong beats. In terry fabrics, the most used thread is made of cotton, aiming to provide water absorption.

Fiber characteristics and properties

Fibers have a molecular structure that contributes to defining their specific properties and characteristics (Table 1), it is these key characteristics that allow their manipulation to create much larger structures, such as yarns.

Table 1: Values of mechanical properties of natural fibers, adapted from Marinelli et al. (2008)

Fiber	Density (g/cm³)	Elongation (%)	Tensile at Break (MPa)	Young's Modulus (GPa)
Cotton	1.5-1.6	7.0-8.0	287-597	5.5-12.6
Flax	1.5	2.7-3.2	345-1035	27.6

Fibers are also blended to obtain qualities that singularly would not be able to be obtained, such as strength, improving the fabric performance, obtaining a unique appearance, and reducing costs (Sinclair, 2014).

Cotton Fiber

Yarn quality parameters such as uniformity, strength, elongation, and fineness are correlated with the length of cotton fibers. The cross-section of cotton fiber is kidney-shaped. The cross-section tends to indicate the relative dimensions of the lumen and fiber walls. Cotton's tenacity and initial modulus are lower compared to hemp fibers, while its elongation at break (5-10%) and its elastic recovery are higher. They are resistant to alkali but degrade by acids (Sfiligoj et al., 2013). Cotton fiber grows from a single seed cell. It is affiliated with the genus *Gossypium Linn*. The main market fibers are *Gossypium barbadense Linn* (known as "Egyptian cotton", the fiber is long and fine), *Gossypium herbaceum Linn* and *Gossypium arboreum Linn* (Indian or Asian, short and coarse fibers), and *Gossypium hirsutum Linn* (it is between Asian and Egyptian cotton fiber, its length and fineness are quite variable). Specifically, upland cotton is a widely cultivated American cotton plant (*Gossypium hirsutum*) having short- to medium-staple fibers. (Laktim, 2018).

Textile manufacturing processes

Yarns: preparation and spinning of textile fibers

Spinning is to transform initially disordered textile fibers into yarns. To spin, it is necessary to prepare the fibers according to their characteristics for each purpose, and each fiber needs a specific preparation. (Piccinini, 2015). Yarns can be spun in different ways, acquiring distinct aspects. Their main twists are the "S" and "Z" depending on the twist direction (clockwise or counterclockwise) and twist level (number of twists per inch or per meter) and the tensile multiplier ($TM = T\sqrt{tex}$) (Scida et al., 2017). A high twist level can cause the decay of the longitudinal strength properties and Young's modulus. Also influence the reduction of air permeability, which can cause the appearance of voids and also influence the drop in properties (Goutianos et al., 2006; Omrani et al., 2017).

Terry fabric

The terry fabric is a fabric with loops on the surface of one or two sides. It can absorb a large amount of water compared to the conventional flat fabric. The terry fabric is looped on one or both sides, usually covering the entire surface or strips. Its edges' finishes include end edges or fringe trims and side edges or selvages. The production of terry fabric is a complex process and is possible only on looms with special equipment. Four threads systems are woven on the terry weaving loom (Figures 1 and 2): ground warp threads, face pile warp threads, back pile warp threads, and weft (or filling) threads. The ground warps threads have a higher tensile while the pile warps threads have a much lower tensile and consequently a longer length, to create the pile loops through the special movement of the loom's reed with soft and strong beats (Singh & Behera, 2015; Yilmaz et al., 2005).

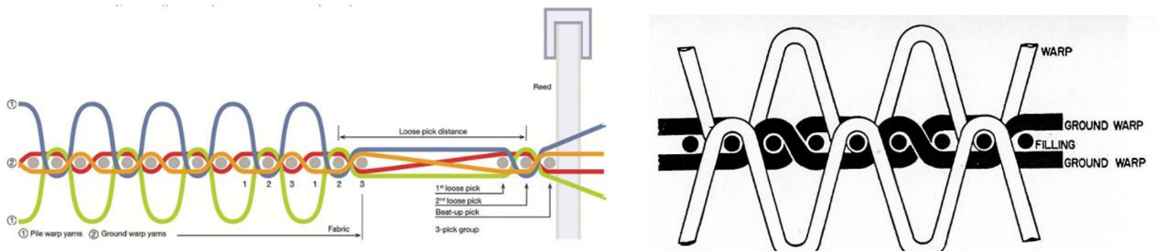

(a) Longitudinal Section of Pile Formation of Three-Pick Terry

(b) Terry Cloth – Pile fabric constructions

Figure 1: Three-Pick Terry Weave (Halawa et al., 2019; Kaswell, 1963)

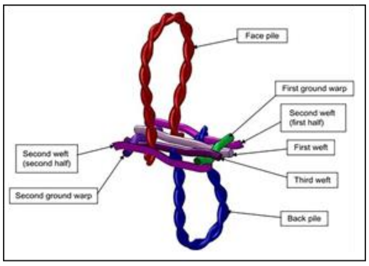

(a) Repeat Unit of Three-Pick Terry Fabric

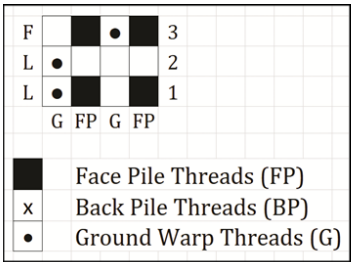

(b) Weave Structure of Three-Pick Terry

Figure 2: Three-Pick Terry Fabric (Halawa et al., 2019)

Among natural fibers, cotton fiber is the most used material for the production of terry fabrics due high absorbency and hypoallergenic properties. An improvement in the production of terry fabrics includes zero-twist threads, which are produced with cotton and PVA fibers. PVA fibers are normally dissolved during the finishing process improving in this way yarn characteristics and performance. The resulting terry fabric is very soft and voluminous, increasing water absorption during use (Cruz et al., 2017; Filiz Sekerden, 2012).

The wetting phenomenon of textile structures involves several primary processes, including immersion, capillary sorption, adhesion, and spreading. During immersion or capillary sorption, the solid-vapor interface disappears and a solid-liquid interface appears. When a drop of liquid is placed on a fabric, it spreads by capillary action. The water absorption of terry fabric increases with increasing pile length (pile height) and area density. The percentage of water absorbed by fabrics with high loop density is greater than that of fabrics with lower loop density (Figure 3). The level of absorption and transport of liquids in a fabric depends on the size of the pores and their distribution. Liquid or water occupies small pores initially and moves to larger pores (Cruz et al., 2017; Petrulyte & Baltakyte, 2008).

(a) Rotor pile terry cloth

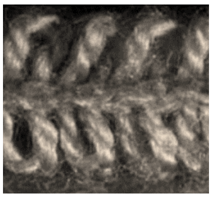

(b) Ring pile terry cloth

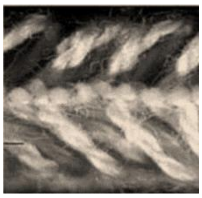

(c) High loop length but low loop density

(d) Low loop length but high loop density

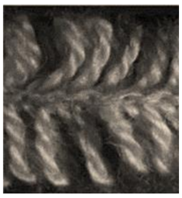

(e) Double ply yarn fabric

(f) Single-layer yarn fabric

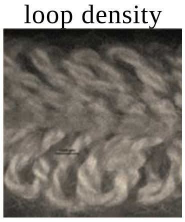

(g) Smaller form factor loops

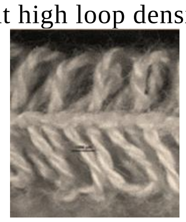

(h) Larger form factor loops

(i) Single-layer yarn terry cloth

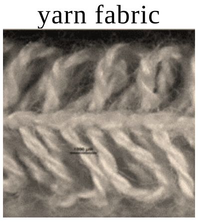

(j) Double ply yarn terry cloth

(l) Zero Twist wires

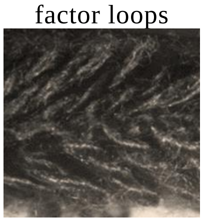

(m) Long fiber bamboo fiber yarn

Figure 3: Cross-sectional view of terry fabric (Singh & Behera, 2015)

The water absorption was related to warp, weft, and pile characteristics. The percentage of water absorption is the lowest for open-ended yarn and the highest for two-layer ring carded yarn. Due to the higher twist and compact structure of the open-end wire, it has less water penetration capability. The water absorption of terry fabrics decreases with increasing warp and weft densities as the fabric structure becomes very compact and dense (Cruz et al., 2017; Petrulyte & Baltakyte, 2008). However, absorption can be improved with an increase in pile height which increases the warp surface area of the pile.

Fabrics for high-performance composites

The increase in environmental awareness stimulated the idea of reducing synthetic-based products in the production of composite materials and more specifically reinforcements. To achieve this goal, the incorporation of cellulosic fibers such as flax, hemp, or kenaf has received attention. Its specific mechanical properties are competitive when compared to glass fibers and have greater environmental benefits (Corbin et al., 2020). Vegetable fibers, when applied correctly, produce a material in which the fibers and the matrix have good adhesion, making it possible to obtain similar or even better mechanical properties than the pure polymer matrix. The issue of natural fiber reinforcement polymers is being researched in several applications (Cordeiro et al., 2022).

In the textile process, there is direct control over the placement of the fibers and the ease of handling the fibers. Natural fiber-reinforced polymer composites are increasingly being used in many engineering applications with an extremely wide range of properties. Textile performance operations play a key role in most composite manufacturing processes. The basic processes of forming textile yarns and fabrics have been significantly modified and developed to meet the growing demand in the composites manufacturing sector. (Chen, 2015; Corbin et al., 2020; Elseify et al., 2019; Omrani et al., 2017).

Cevallos & Olivito (2015) quantified the effects of the mechanical properties of the fabrics on the tensile behavior of composites reinforced with natural fabric and glass, properties such as tensile strength, Young's modulus, and deformation to failure were considered. The mechanical properties of the fabrics used in this study are presented and compared with those of cementitious composites produced with a layer of fabric strips. In Table 2, the data are grouped according to the type of fabric, with a comparative analysis of stiffness and strength values, the tensile strength, and stiffness per unit width (N/mm) of the composites evaluated considering the method for impregnated systems (Cevallos Velàsquez, 2014).

Table 2: Tensile properties of fabric strips and fabric-reinforced cementitious composites (Cevallos & Olivito, 2015).

Composites (IS)	Tensile properties of fabrics				Tensile properties of composites (one layer)					
	σ_f (MPa)	$\sigma_f.t_f$ (N/mm)	$E_f.t_f$ (N/mm)	ε_f (%)	σ_U (MPa)	$\sigma_U.t_U$ (N/mm)	$E_U.t_U$ (N/mm)	ε_I (%)	ε_{II} (%)	ε_{III} (%)
Flax fabric composites	292.23	31.57	404.76	11.009	196.55	21.23	2.16	0.038	6.199	12.157
Sisal fabric composites	249.16	31.45	550.90	7.872	176.37	22.26	5.05	0.032	3.223	7.918
Glass fabric composites	2900.00	356.92	8738.46	4.500	360.16	44.33	81.23	0.034	-	0.842

Where:

σ_f = tensile strength of fabrics,
$t_f = A_f/b_f$, b and t are
the composite width and thickness,
$\sigma_f.t_f$ = tensile strength per unit width of fabrics,
$E_f.t_f$ = Young's modulus per unit width of fabrics,
ε_f = strain to failure of fabrics.

σ_U = ultimate tensile strength of composites,
$\sigma_U.t_U$ = tensile strength per unit width of composites,
$E_U.t_U$ = Young's modulus per unit width of composites (third stage),
ε_I, ε_{II}, ε_{III} = strain capacity of composites at first, second and third stages, respectively.

Terry fabrics could be used in the development of composites with a larger contact area between matrix and reinforcement, due to their vertical and horizontal access structure of the sheet, thus increasing strength. Although terry fabrics were mentioned in passing in the review paper about potential fabric-reinforced composites (Hasan et al., 2021), the present authors did not find in the literature research related to the effective use of terry fabrics in composites.

In this way, this research aimed to the characterization of terry fabrics focused on the potential for utilization as reinforcing elements in engineered composites. The specific objectives were to analyze: (1) optical microscopy to differentiate ligament and loop structures; (2) tensile and tear strength analysis (3) DIC analysis to check strain/stress points on the X and Y axis before fabric rupture.

MATERIALS AND METHODS

Materials

Terry fabrics were selected according to the type of fiber and fabrics with different loops and interlacing structures. For analysis, the terry fabrics were not washed for the characterization tests (analyzed as supplied by the companies). In this study, they were named: **Material 1** – terry fabric made from 100% Egyptian cotton and **Material 2** - terry fabric made from 100 % upland cotton.

Methods

Concerning the methods selected to characterize and define the strength of the terry flat fabrics, they were: determination of the yarn count; thickness; weight; optical microscopy; Grab tensile test; Elmendorf strength test; and Digital Image Correlation (DIC).

Yarn count number

Standard ABNT NBR 13216:1994 - Textile materials - Determination of yarn count in short-length samples was employed. Tex system was chosen to express textile count. In the process, warp and weft yarns were removed from the terry fabrics, resulting in a total of 300 cm from each Material (1 and 2). They were acclimatized according to the ABNT NBR ISO 139: 2008 Textiles - Atmospheres - standard for conditioning and testing, employing Climatic Chamber with Relative Humidity and Temperature control (MTB Scientific brand), 20ºC temperature and humidity control ranging from 51 to 60%, and immediately weighed on an analytical scale (model Marte - AY Series - Shimadzu AY220 - Capacity/division: 220g/ 0.1mg).

Thickness

Standard ABNT NBR 13371:2005- Textile Materials - Thickness Determination was employed. A portable analog thickness gauge was used, also known as a thickness meter (Mainard brand) with a proximate reading of 0.01 mm. From each Material (1 and 2), 5 measurements were performed (taken diagonally from the selvage border, but excluding it).

Weight

Standard ABNT NBR 10591:2008 - Textile materials - Determination of the weight of textile surfaces was employed, which determines the weight of the plain fabric or knitting, identifying mass per unit area. From each Material (1 and 2), 5 specimens were removed from the terry fabrics (5cm² each) (taken diagonally from the selvage border, but excluding it). They were acclimatized according to the ABNT NBR ISO 139: 2008 Textiles - Atmospheres - standard for conditioning and testing, employing Climatic Chamber with Relative Humidity and Temperature control (MTB Científica brand), 20ºC temperature and humidity control ranging from 51 to 60%, and immediately weighed on an analytical scale (model Marte - AY Series - Shimadzu AY220 - Capacity/division: 220g/ 0.1mg).

Optical Microscopy

From each Material (1 and 2), a 100 mm² area was taken. The test was carried out according to the standard ABNT NBR 13 538:1995. Textile Material – Qualitative analysis. The fiber and fabric were analyzed by optical microscopy of longitudinal and transversal sections. The longitudinal and transversal views were performed in a stereo microscope (Leica, model MS5, Germany) coupled with a video camera for digital image capture (Vista, Protos IV, model VPC 122/CH, 1/2" CCD, Great Britain). The magnifications correspond to 20, 32, 51, 80, and 128 times. The images were captured and processed by the Video Analyzer 2000 code 250 (Mesdan, Italy) (Berlin, 2014; Cattani, 2016). Fibers' diameters, terry fabrics' ligaments, and the type of structure of the fabric ligament were determined. The tests were performed at the Textile Fibers Laboratory, School of Arts, Sciences, and Humanities of University of São Paulo (EACH-USP) (São Paulo, SP, Brazil).

Grab Tensile Test

From each Material (1 and 2), 5 samples were obtained in the weft direction and 5 samples in the warp direction of each product (taken diagonally from the selvage border, but excluding it). Each sample presented dimensions of 75 x 100 mm. The test was carried out according to the standards ABNT NBR ISO 13934-1: 2016 - Textiles — Tensile properties of fabrics - Part 1: Determination of maximum strength and elongation at maximum strength using the strip method and ABNT NBR ISO 13934-2: 2016 - Textiles — Tensile properties of fabrics - Part 2: Determination of strength maximum using the grab test method, and the samples were previously acclimatized according to NBR ISO 139 (described above). A servo-hydraulic machine, model 370.02, manufacturer MTS, (Figure 4(a)) load of 1kN and a speed of 20 mm/min was used. For each test, the software generated values of strength (N), tensile stress (MPa), elongation (mm), specific deformation (mm/mm), percentage deformation (%), and elastic modulus (MPa) calculated from the other values.

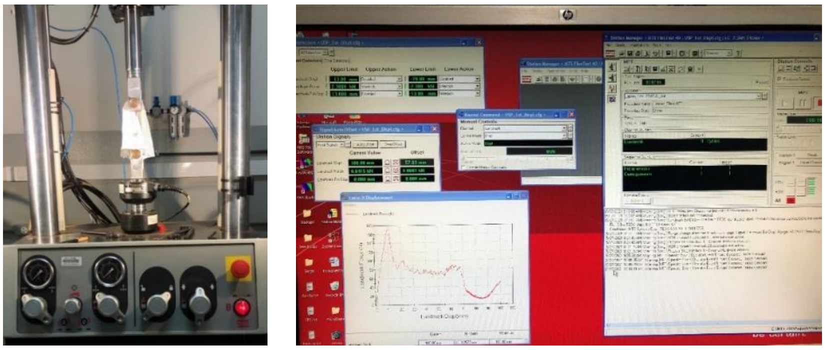

(a) (b)

Figure 4: Grab Tensile Test.

The Station Manager - MTS Flextest 40 software (Figure 4b) of the tester machine-generated values of strength (N), tensile strength (MPa), and specific deformation (mm/mm). The values of elongation (%) are calculated from Eq. 1.

$$\varepsilon = \left(\frac{L_f - L_0}{L_0}\right) x\ 100\ \% \quad \text{Eq. 1}$$

Where:

ε = elongation (%)

L_0 = Original Length

L_f = Length of the sample after stretching

The value was the ratio of the stress of the material to the corresponding strain. The calculation formula was as follows in Eq. 2:

$$E = \frac{\sigma}{\varepsilon} = \frac{F.L_0}{A.\Delta L} \qquad \text{Eq. 2}$$

Where:
E = each fabric sample was solved by curve fitting
σ = tensile stress
ε = elongation
F = tensile load
L_0 = Original Length
A = cross-sectional area of the sample
ΔL = tensile displacement of the sample.

The tests were performed at the Laboratory of Rural Constructions and Ambience, Faculty of Animal Science and Food Engineering of University of São Paulo (FZEA-USP) (Pirassununga, SP, Brazil).

Elmendorf tear strength test

From Material 1 and 2 terry fabrics, 3 samples in the weft direction and 3 samples in the warp direction were taken diagonally from the selvage border, but excluding it. They did not contain the same longitudinal or transverse threads or were not cut within 150 mm of the fabric edge. Each sample presented dimensions of 75 x 100 mm. The tests were carried out according to the standard ABNT NBR ISO 13937-1: 2021 - Textiles — Tear Properties of Fabrics - Part 1: Determination of Tear Strength Using the Ballistic Pendulum Method (ELMENDORF). It was used an electronic Elmendorf machine, model HTF-018 manufacturer HTI, load from 1 to 3 kN and intermediate scale. The tests were performed at the Textile Analysis Laboratory of the Golden Technology company (São José dos Campos, SP, Brazil).

Digital Image Correlation – DIC

The DIC test was performed together with the Grab Tensile test to generate the images of the highest stress before and after the rupture of the samples. The samples were taken from Material 1 and 2 terry fabrics (from each one, 1 sample in the weft direction and 1 sample in the warp direction). They presented dimensions of 10 x 7.5 cm) and acclimatized (20ºC temperature and humidity control ranging from 51 to 60%). Also, they were stamped by Stamp Rollers (Correlated Solutions brand) to generate the correlation points – Figure 5.

(a) stamp and ink box (b) stamp roll (c) stamped sample

Figure 5: Stamp Rollers

Equipment assembly, camera calibration, and the average, minimum, and maximum magnification in the calibration volume for the two cameras are shown in Figure 6.

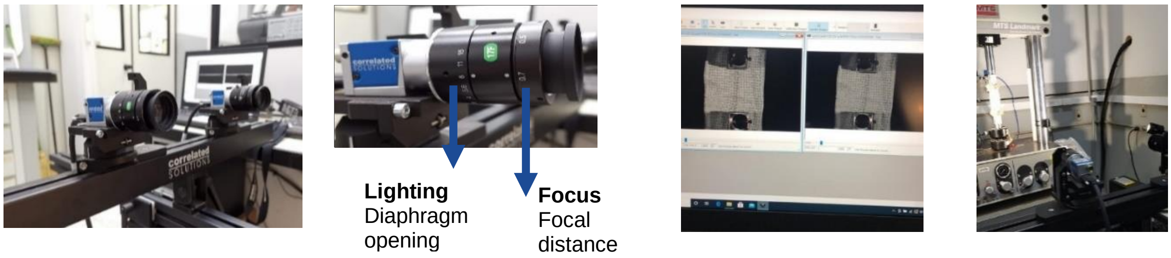

(a) Camera positioning (b) Setting the lighting and focus (c) Image of the cameras with lighting and the focus set (d) DIC Test Assembly with Pull Test Grab

Figure 6: Assembly of DIC equipment

Interest images generated by the left and right cameras, respectively, are shown in Figure 7a. The range of the interest area used for correlation analysis is shown in Figure 7b.

(a) Reference speckle images (b) Interest area used for correlation analysis

Figure 7: Reference speckle images and area of interest

The images were obtained using the equipment VIC-3D – System by Correlated Solutions. Analyzes and images of DIC test results in the "VIC-3D 9 System" software are presented in the results and discussion. The tests were performed at the Laboratory of Rural Constructions and Ambience, Faculty of Animal Science and Food Engineering of University of São Paulo (FZEA-USP) (Pirassununga, SP, Brazil).

RESULT AND DISCUSSION

Yarn count (Tex), Thickness (mm), and Weight (g/m^2)

The results were shown in Table 3. The thicker yarns were the ones with the highest count numbers, which also provide thicker fabrics. The count number of flat fabric yarns with piles presents a higher numbering in terry fabrics than in simple flat fabrics. The pile yarns present less twist and may reflect on the yarn mass; as higher the count number, as better the water absorption of the terry fabric. Therefore, Material 1 presents a higher count number and probably higher absorption than Material 2. In addition, Material 1 presents greater thickness and weight than Material 2, which also can provide the feeling of greater absorption for this type of article.

Table 3: Yarn count (Tex), Thickness (mm), and Weight (g/m^2)

Terry fabrics	Yarn count (Tex)	Thickness (mm)	Weight (g/m^2)
Material 1 – 100% Egyptian cotton	47 PW / 45 GW / 42 F	2.7	542.72
Material 2 – 100 % upland cotton	40 PW / 33 GW / 44 F	1.44	311.84

PW –pile warp, GW – ground warp, and F – filling (or weft)

Optical Microscopy

Longitudinal and transversal microscopy are shown in Figure 8.

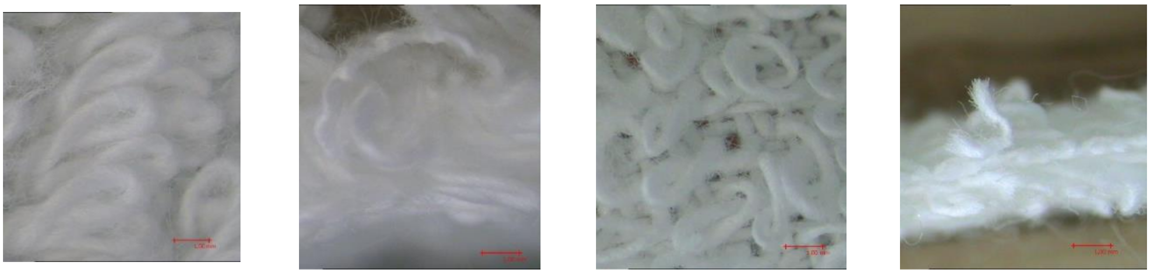

(a) Material 1 - longitudinal

(b) Material 1 - transversal

(c) Material 2 - longitudinal

(d) Material 2 - transversal

Figure 8: Longitudinal and transversal optical microscopy (20x magnification and 1.00 mm scale).

It is possible to observe that the structure of the loops is different: Material 1 (Figure 8 (c) and (d)) present loops (piles) with sharper threads or more twisted threads, and Material 2 (Figure 8 (a) and (b)), loops with more open yarns or with less yarn twist. Material 2 presents opener ligaments (representing opener loops and fabric structure).

Grab Elmendorf tear strength tests (weft and warp)

For the Grab test, the tensile curves (MPa) versus specific deformation (%) are exemplified in Figures 9a and 9c (tests performed in the weft direction) and Figures 9b and 9d (tests performed in the warp direction).

In both cases, it is noticed that the curves rise to a maximum value of tensile strength (which corresponds to the maximum fabric tear strength) followed by a zigzag line that corresponds to the thread-to-thread tearing of the fabric until the total separation into two pieces at the end of the test. At this point, the maximum deformation value is greater than 100% due to the deformation of the fabric until its separation into two parts.

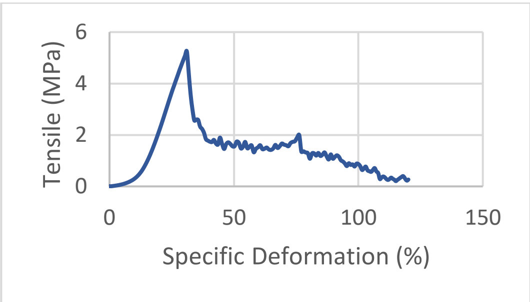

(a) Material 1 - Weft direction

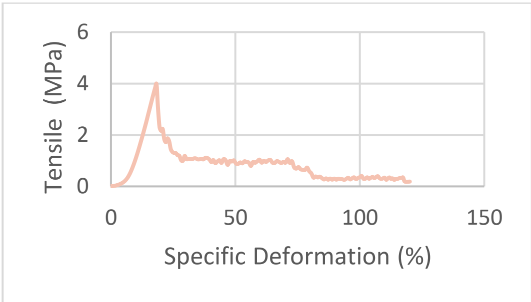

(b) Material 1 - Warp direction

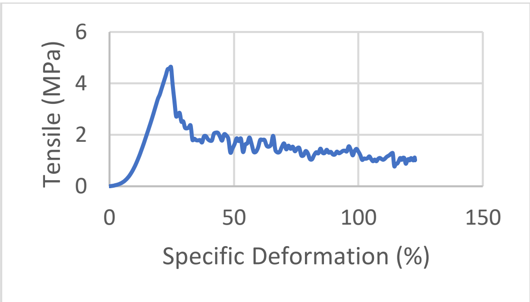

(c) Material 2 - Weft direction

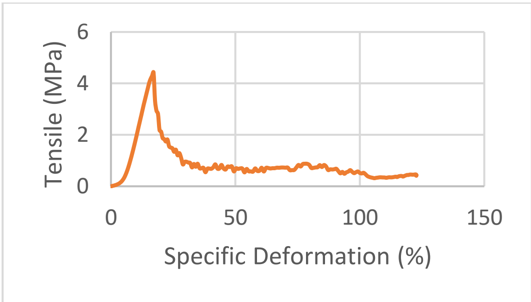

(d) Material 2 - Warp direction

Figure 9: Grab tests – exemplificative curves of stress (MPa) versus specific strain (%) for Material 1 and Material 2.

The values of the maximum tensile stress (MPa) and Elastic Modulus - MOE (MPa) are presented in column chart format respectively in Figures 10(a), 10(b), 10(c), and 10(d).

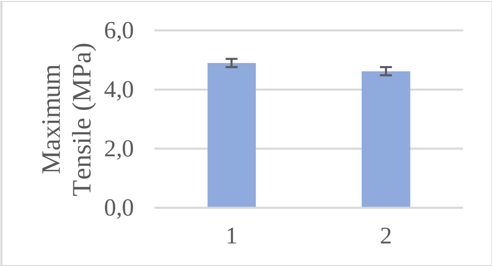

(a) Tensile stress (MPa) - weft direction

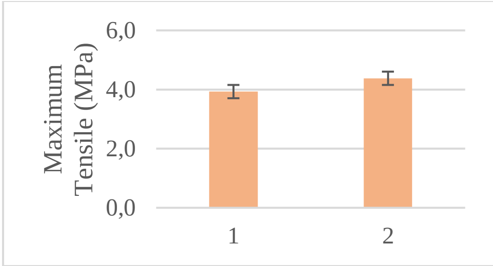

(b) tensile stress (MPa) - warp direction

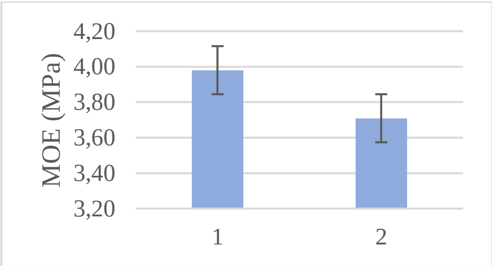

(c) Elastic Modulus - MOE (MPa) - weft

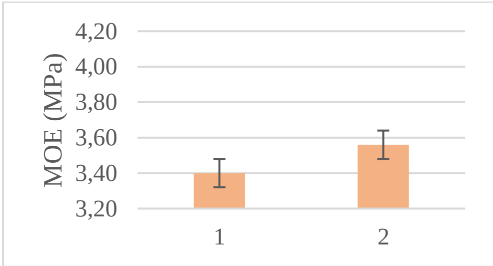

(d) Elastic Modulus - MOE (MPa) - warp

Figure 10: Grab tests - maximum tensile strength (MPa) and Elastic Modulus - MOE (MPa) - (1) Material 1, and (2) Material 2.

Generally speaking, textile materials are expected to have higher values of maximum tensile strength in the warp direction compared to the weft direction since there are generally more yarns per linear centimeter in the warp direction than in the weft direction. However, in the present case, the structure of weft and warp in terry fabric is different than in conventional flat fabrics, which may affect the results of maximum tensile strength in the weft and warp direction. It is observed that in terry fabrics, the loop structure is present in the warp and that, for each terry fabric, there is a different loop structure.

It is identified in the comparison of Figure 10(a), the result of maximum tensile strength in the weft direction Material 1 is greater than Material 2, and in Figure 10(b), in the warp direction, Material 2 has the maximum tensile strength greater than Material 1. In Figure 10(c), the Modulus of Elasticity (MOE) results in the weft direction of Material 1 is much higher than in Material 2. In the warp direction (Figure 10(d)) the Modulus of Elasticity (MOE) values in Material 2 are much higher than in Material 1.

Material 1 is composed of 100% Egyptian cotton, which, due to its longer and finer fibers, allows the production of highly cohesive and high-resistance yarns. Still in the comparison of Figures 10(c) and 10(d), it can be observed that the results of Modulus of Elasticity (MOE) in the warp direction are different from those observed in the weft direction. Although both samples have the same composition (100% cotton), what may be more influencing this behavior is the structure of the loop and the number of warp yarns, since in all towels there is a different structure of loops, yarns, and fibers.

The terry fabric Material 2 has greater resistance in the warp direction due to the greater number of twists shown in Figure 8, and as greater the number of twists of the yarn, as greater its resistance, regardless of the fiber type. The higher strength of the terry fabric Material 1 is higher in the weft direction, because of its type of longer fiber, which increases the strength, even if it has the same twist as other fibers. The most relevant values for the analysis - maximum strength (N), tensile strength

(MPa), deformation at maximum strength (%), and Elmendorf tear resistance test - are presented in Table 4 in the direction of weft and warp.

Table 4 - Maximum strength (N), Tensile stress (MPa), Deformation at maximum strength (%), and Elmendorf tear strength (N).

Terry fabrics	Test Direction	Maximum strength (N)	Tensile stress (MPa)	Deformation at maximum strength (%)	Elmendorf tear strength (N)
Material 1 - 100% Egyptian cotton	Weft	330.57±56.39 (CV=17.1%)	4.90±0.84 (CV=17.1%)	35.98±4.24 (CV=11.8%)	94.4
	Warp	233.56±79.52 (CV=34.0%)	3.46±1.18 (CV=34.0%)	17.98±1.97 (CV=11.0%)	48.53
Material 2 - 100 % upland cotton	Weft	166.33±7.22 (CV=4.3%)	4.62±0.20 (CV=4.3%)	19.25±5.10 (CV=26.5%)	52.6
	Warp	157.68±8.91 (CV=5.7%)	4.38±0.25 (CV=5.7%)	18.16±3.36 (CV=18.5%)	24

Table 4 shows the tear resistance of the fabrics. Material 2, with composition (100% upland cotton), presents the lowest tear strength. On the other hand, the highest value strength is presented by Material 1, which is made up of 100% Egyptian cotton and whose fiber type and weaving structure can be related to this result.

Digital Image Correlation – DIC

In the DIC test, the objective is the image correlation for shape, motion, and deformation of the samples before the breaking point on the Grab tensile test. This test presents good results in plain fabrics, due to the good absorption of the stamp ink and a flatter texture (Figure 5).

DIC (Weft)

The links to access the complete videos are shown in Table 5.

Table 5: Links to access the Grab and DIC Tensile test videos in the weft direction.

Description of terry fabrics – Weft	Link to access the DIC test videos
(a) Material 1 - 100% Egyptian cotton	https://youtu.be/XJ7oQZiR7lY
(b) Material 2 - 100 % upland cotton	https://youtu.be/K_Q3sSoYsi0

The test of samples in the weft direction (Table 5) presents the collected images related to Grab tests (Table 3 and Figure 9).

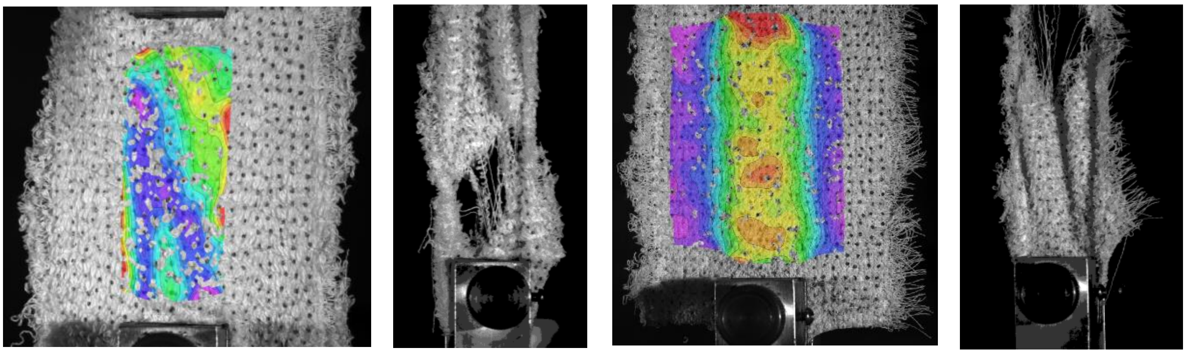

(a) Material 1 (b) Material 1 (c) Material 2 (d) Material 2

Figure 11: (a) and (c) Stress stain of fabrics in the weft direction - (b) and (d) Photo at the moment of fabric rupture in the weft direction.

Figures 11 (a) and (c) show the major strain areas. The red regions are the areas of greatest stress, which are likely to be the fabric break points. The photos in Figures 11 (b) and (d) show the tearing of each fabric, which coincides with the stress points shown in Figures 11 (a) and (c). In Figures 11 (c) and (d), the rupture is closer to the upper jaw. Meanwhile, for the Material 1 fabric, represented by Figures 11 (a) and (b), the points to the central rupture are close to the lower jaw, different from Material 2. Material 1 presented the highest strength and maximum tensile strength in the Grab test (Table 3).

DIC (Warp)

The test of samples in the warp direction (Table 6) presents sharpness in the collected images (Figures 11 and 12) and also are related to Grab tests (Table 3 and Figure 9).

Table 6: *L*ink*s* to access the Grab and DIC Tensile test videos in the warp direction.

Description of terry fabrics - Warp	**Link to access the DIC test videos**
(a) Material 1 - 100% Egyptian cotton	https://youtu.be/W6Bi3SupjS8
(b) Material 2 - 100 % upland cotton	https://youtu.be/2KEKYqBayDg

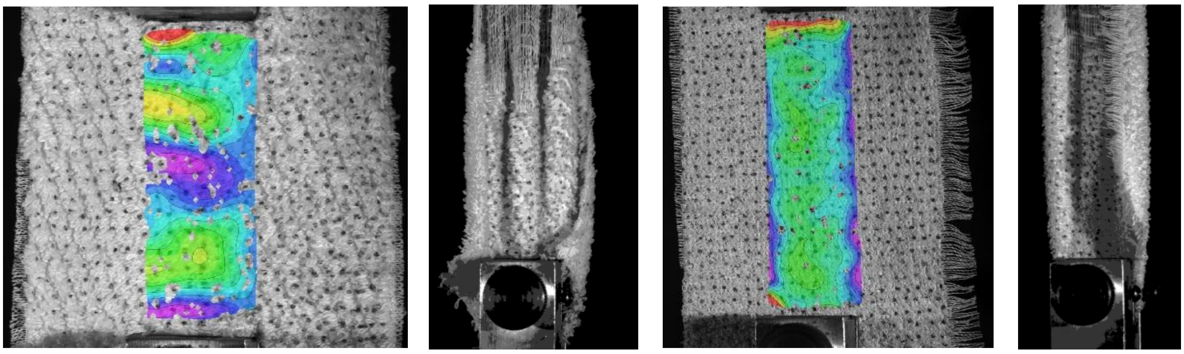

(a) Material 1 (b) Material 1 (c) Material 2 (d) Material 2

Figure 12: (a) and (c) Stress stain of fabrics in the warp direction - (b) and (d) Photo at the moment of fabric rupture in the warp direction.

Figures 12 (a) and (c) show the major strain areas. The red regions are the areas of greatest stress, which are likely to be the fabric break points. The photos in Figures 12 (b) and (d) show the tearing of each fabric, which coincides with the stress points shown in Figures 12 (a) and (c). In Figures 12 (c) and (d), the rupture is closer to the jaws. Meanwhile, for the Material 1 fabric represented by Figures 12 (a) and (b), the points to the central rupture are close to the upper jaw, different from Material 2. Material 1 presented the highest strength and maximum tensile strength in the Grab test (Table 3).

CONCLUSION

The study started from the demand to identify the analysis of terry flat fabrics in the segment of unconventional materials for technical employment. The present article was focused on the analysis of these properties in terry fabrics produced in Brazil.

Two terry fabrics available in the Brazilian market were selected, varying cotton fiber and fabric structure, provided by different suppliers: Material 1 - 100% Egyptian cotton (2.7 mm thickness and 543 g/m² weight) and Material 2 - 100 % upland cotton (1.4 mm thickness and 312 g/m² weight).

The fabrics were acclimatized and subjected to tensile strength testing along with DIC (Digital Image Correlation). From Material 1 and Material 2, five specimens were separated, in the warp and weft direction, and the DIC was performed on the first specimen of each sample, in addition to performing the optical microscopy analysis to verify the fabric ligament structure, twist of the threads, and loops (piles). The obtained results were:

(1) concerning optical microscopy, Material 1 presented its tighter ligament, the loops as well and the yarn structure presents a more voluminous appearance, being possible to consider less torsion than Material 2, which presents opener ligaments (representing opener loops and fabric structure);
(2) Material 1 presented lower tensile stress in the warp direction (3.5 MPa) than Material 2 (4.4 MPa). In the weft direction, Material 1 presents greater tensile stress (4.9 MPa) than Material 2 (4.6 MPa). Regarding the modulus of elasticity, Material 1 presented a lower tensile value in the warp direction (3.4 MPa) than Material 2 (3.6 MPa), whereas, in the weft direction, Material 1 presents a higher tensile value (4.0 MPa) than Material 2 (3.7 MPa). In Elmendorf the tear strength test, Material 1 (weft: 94.4 N and warp: 48.5 N) presents greater values than Material 2 (weft: 52.6 N and warp: 24 N) in both directions. In addition, in the last case, weft direction values in both Materials were greater than in the warp direction;
(3) Material 1 presented inferior central breaking points in the weft direction and the upper jaws in the warp direction. Material 2 showed break points in the upper jaws in the weft and warp directions; DIC presents the most prominent tensile strength in the green and red colors, and in the warp direction, corresponding to at the top end and in the weft direction (analyzed interest area was larger, as it did need more reference points for the formation of image and stress points), and presented the greatest stress in the central region of the interest area;

For future studies, composites with terry fabric reinforcements and further tests for evaluation of the contact area should be carried out.

ACKNOWLEDGEMENT

The work presented in this article was partially funded by FAPEMIG (Research Support Foundation of the State of Minas Gerais) and CAPES (Higher Education Personnel Improvement Coordination).

CONFLICT OF INTEREST

The authors declare that they have no conflicts of interest associated with the work presented in this paper.

DATA AVAILABILITY

Data on which this paper is based is available from the authors upon reasonable request.

REFERENCES

ABNT NBR 10 588:2015. Flat fabrics — Determination of yarn density. Brazilian Association of Technical Standards. ABNT 7p.

ABNT NBR 10 591:2008 - Textile materials - Determination of the weight of textile surfaces. Brazilian Association of Technical Standards. 4p.

ABNT NBR 13 371:2005- Textile materials - thickness determination. Brazilian Association of Technical Standards. 11p.

ABNT NBR 13 538: 1995. Textile Material – Qualitative analysis. Brazilian Association of Technical Standards. ABNT 20p.

ABNT NBR ISO 13 934-1:2016 - Textiles — Tensile properties of fabrics - Part 1: Determination of maximum strength and elongation at maximum strength using the strip method. Brazilian Association of Technical Standards. 18p.

ABNT NBR ISO 13 934-2:2016 - Textiles — Fabric tensile properties - Part 2: Determination of maximum strength using the Grab test method. Brazilian Association of Technical Standards. 16p.

ABNT NBR ISO 13 937-1: 2021- Textiles — Tear properties of fabrics - Part 1: Determination of tear strength using the ballistic pendulum method (ELMENDORF). Brazilian Association of Technical Standards. 17p.

ABNT NBR ISO 139:2008. Textiles – Normal test conditioning atmospheres. Brazilian Association of Technical Standards. 6p.

Berlin, G. (2014). A Indústria têxtil brasileira e suas adequações na implementação do desenvolvimento sustentável. *Modapalavra E-Periódico*, *7*(13), 15–45.

Cattani, I. M. (2016). *Fibra de Buriti (Mauritia flexuosa Mart.): registro em comunidade local(Barreirinhas-MA, Brasil), caracterização físico-química e estudo comimpregnação com resinas* [Universidade de São Paulo]. https://doi.org/10.11606/D.100.2016.tde-29092016-100227

Cevallos, O. A., & Olivito, R. S. (2015). Effects of fabric parameters on the tensile behaviour of sustainable cementitious composites. *Composites Part B: Engineering*, *69*, 256–266. https://doi.org/10.1016/j.compositesb.2014.10.004

Cevallos Velàsquez, O. A. (2014). *Sustainable fabric-reinforced cementitious composites for the strengthening of masonry elements*. University of Calabria.

Chen, X. (2015). Advances in 3D Textiles. In Xiaogang Chen (Ed.), *Elsevier* (1st ed.). Woodhead Publishing Limited in Association with The Textile Institute.

Corbin, A. C., Soulat, D., Ferreira, M., Labanieh, A. R., Gabrion, X., Malécot, P., & Placet, V. (2020). Towards hemp fabrics for high-performance composites: Influence of weave pattern and features. *Composites Part B: Engineering*, *181*(October 2019). https://doi.org/10.1016/j.compositesb.2019.107582

Cordeiro, A. O. T., Laktim, M. C., Kohan, L., Baruque-Ramos, J., Fangueiro, R., de Castro Engler, R., & Martins, C. R. (2022). Cotton Weaving Waste Incorporation in PVC Composites. *Materials Circular Economy*, *4*(1), 1–10. https://doi.org/10.1007/s42824-022-00061-7

Cruz, J., Leitão, A., Silveira, D., Pichandi, S., Pinto, M., & Fangueiro, R. (2017). Study of moisture absorption characteristics of cotton terry towel fabrics. *Procedia Engineering*, *200*, 389–398. https://doi.org/10.1016/j.proeng.2017.07.055

Elseify, L. A., Midani, M., Shihata, L. A., & El-Mously, H. (2019). Review on cellulosic fibers extracted from date palms (Phoenix Dactylifera L.) and their applications. *Cellulose*, *26*(4), 2209–2232. https://doi.org/10.1007/s10570-019-02259-6

Filiz SEKERDEN. (2012). Investigation of water absorbency and color fastness of modal woven towels. *Scientific Research and Essays*, *7*(2), 145–148. https://doi.org/10.5897/sre11.804

Goutianos, S., Peijs, T., Nystrom, B., & Skrifvars, M. (2006). Development of flax fiber-based textile reinforcements for composite applications. *Applied Composite Materials*, *13*(4), 199–215. https://doi.org/10.1007/s10443-006-9010-2

Halawa, O. E., Osama, P., & Halawa, E. (2019). *Three-Dimensional Design of Terry Fabrics Three-Dimensional Design of Terry Fabrics Abstract : 9*(3).

Hasan, K. M. F., Horváth, P. G., & Alpár, T. (2021). Potential fabric-reinforced composites: a comprehensive review. *Journal of Materials Science*, *56*(26), 14381–14415. https://doi.org/10.1007/s10853-021-06177-6

Kaswell, E. R. (1963). *Wellington Sears Handbook of Industrial Textiles.* Wellington Sears Co; First Edition.

Laktim, M. C. (2018). *Cama, mesa e banho: desenvolvimento de materiais e processos têxteis, design e moda no Brasil (1976 - 2017)* [Universidade de São Paulo]. https://doi.org/10.11606/D.100.2018.tde-31102018-172203

Omrani, F., Wang, P., Soulat, D., & Ferreira, M. (2017). Mechanical properties of flax-fibre-reinforced preforms and composites: Influence of the type of yarns on multi-scale characterisations. *Composites Part A: Applied Science and Manufacturing*, *93*, 72–81. https://doi.org/10.1016/j.compositesa.2016.11.013

Petrulyte, S., & Baltakyte, R. (2008). Investigation into the wetting phenomenon of terry fabrics. *Fibres and Textiles in Eastern Europe*, *16*(4), 62–66.

PICCININI, L. (2015). *Um estudo do processo de desenvolvimento de produto no vestuário de moda na malharia retilínea no Brasil* [Universidade de São Paulo]. https://www.teses.usp.br/teses/disponiveis/100/100133/tde-23112015-170607/publico/CorrigidaLAURAPICCININI.pdf

Scida, D., Bourmaud, A., & Baley, C. (2017). Influence of the scattering of flax fibers properties on flax/epoxy woven ply stiffness. *Materials and Design*, *122*, 136–145. https://doi.org/10.1016/j.matdes.2017.02.094

Sfiligoj, M., Hribernik, S., Stana, K., & Kree, T. (2013). Plant Fibres for Textile and Technical Applications. In *Advances in Agrophysical Research* (p. 13). InTech. https://doi.org/10.5772/52372

SINCLAIR, R. (2014). *Textiles and fashion: materials, design and technology* (R. Sinclair (ed.); 1st ed.). Elsevier. https://books.google.com.br/books?hl=pt-BR&lr=&id=GJlzAwAAQBAJ&oi=fnd&pg=PP1&dq=SINCLAIR,+R.+Textiles+and+Fashion:+Materials,+Design+and+Technologies.+Cambridge:+Woodhead+Publishing,+2014.+913+p.+&ots=DlJkCgygzy&sig=F7bGw59pvNbjQBCL5i9B4zyvPHk#v=onepage&q

Singh, J. P., & Behera, B. K. (2015). Performance of terry towel. *Indian Journal of Fibre and Textile Research*, *40*(1), 112–121.

Yilmaz, N. D., Powell, N. B., & Durur, G. (2005). The technology of terry towel production. *Journal of Textile and Apparel, Technology and Management*, *4*(4), 115–160. https://www.scopus.com/record/display.uri?eid=2-s2.0-32544438016&origin=resultslist